G. L. Gray
Assistant Professor,
Department of Engineering
Science and Mechanics,
The Pennsylvania State University,
University Park, PA 16802
Assoc. Mem. ASME.

I. Dobson
Associate Professor,
Department of Electrical and
Computer Engineering.

D. C. Kammer
Associate Professor,
Assoc. Mem. ASME.
Department of Engineering Mechanics
and Astronautics.

University of Wisconsin–Madison,
Madison, WI 53706

Chaos in a Spacecraft Attitude Maneuver Due to Time-Periodic Perturbations

We use Melnikov's method to study the chaotic dynamics of an attitude transition maneuver of a torque-free rigid body in going from minor axis spin to major axis spin under the influence of small damping. The chaotic motion is due to the formation of Smale horseshoes which are caused by the oscillation of small subbodies inside the satellite. The equations of motion are derived and then transformed into a form suitable for the application of Melnikov's method. An analytical criterion for chaotic motion is derived in terms of the system parameters. This criterion is evaluated for its significance to the design of artificial satellites.

1 Introduction

This paper deals with the dynamics of an attitude transition from minor to major axis spin[1] of a quasi-rigid, single-body spacecraft perturbed by small oscillating subbodies. A single-body satellite is directionally unstable in the presence of energy dissipation when perturbed from spinning about its minor axis (Hughes, 1986). In the absence of active stabilization, the body will eventually reorient itself and spin about the major axis. Oscillating subbodies can produce chaos in a region of the phase space traversed by the satellite during this attitude maneuver. This maneuver is of great practical interest since the initial rotation of many spacecraft is about their minor axis after launch vehicle separation. The addition of oscillating subbodies allows for simple modeling of perturbations within the carrier body. These perturbations might include: asymmetric rotors, reciprocating engines, and crew movement within the vehicle. It should be noted that we prove the existence of horseshoes, which imply the existence of chaotic transients (Greenspan and Holmes, 1983; Guckenheimer and Holmes, 1983). Therefore, throughout this work, when we refer to chaos or chaotic dynamics, we are generally referring to transient chaos and not the chaos associated with a strange attractor.

Certain aspects of the dynamics of attitude transition maneuvers have been studied for the special class of spacecraft called dual-spin satellites. These satellites are reoriented by spin-up of rotors relative to the main spacecraft body. Attitude resonances in this maneuver, occurring during the spin-up or spin-down, have been investigated using perturbation techniques and numerical simulation (Adams, 1980; Cochran and Holloway, 1980; Gebman and Mingori, 1976; Hall and Rand, 1991; Or, 1991). In the case of single-body satellites, the direction and control of the final major axis orientation have been studied by authors such as Barba et al. (1973), Cronin (1978), Kaplan and Cenker (1973), and Rahn and Barba (1991), but the dynamics of the maneuver itself have not been extensively investigated.

The non-Hamiltonian perturbations of rigid-body dynamics dealt with in this paper are due to time-periodic enforced motions of subbodies within a satellite possessing an energy dissipation mechanism. While the occurrence of chaos in this class of systems is not surprising, our application of Melnikov's method to detect the onset of chaos in this class of systems is new. We have overcome considerable difficulties in model formulation and in the application of Melnikov's method to obtain a criterion for chaos which can be used in satellite design. The most closely related work (Dovbysh, 1989; Holmes and Marsden, 1983; Koiller, 1984; Ziglin, 1982) is limited to

[1] In this work, the minor axis corresponds to the principal axis with the smallest mass moment of inertia, while the major axis denotes the principal axis with the largest inertia.

Contributed by the Applied Mechanics Division of THE AMERICAN SOCIETY OF MECHANICAL ENGINEERS for publication in the ASME JOURNAL OF APPLIED MECHANICS.

Discussion on this paper should be addressed to the Technical Editor, Professor Lewis T. Wheeler, Department of Mechanical Engineering, University of Houston, Houston, TX 77204-4792, and will be accepted until four months after final publication of the paper itself in the ASME JOURNAL OF APPLIED MECHANICS.

Manuscript received by the ASME Applied Mechanics Division, Dec. 4, 1992; final revision, Sept. 3, 1993. Associate Technical Editor: D. J. Inman.

chaos in satellite attitude dynamics when the perturbations are Hamiltonian. Some work has been done for non-Hamiltonian perturbations to spacecraft dynamics, but it has dealt almost exclusively with the stability of equilibria (Baillieul and Levi, 1987; Krishnaprasad, 1985; Krishnaprasad and Marsden, 1987; Rubanovskii, 1988). In particular, the non-Hamiltonian perturbations studied in this work are explicit functions of time, resulting in equations of motion with time-dependent coefficients. This type of perturbation is of considerable practical importance in satellite design. For example, the enforced time-dependent motion, modeled herein by harmonic functions of the form $A \cos \Omega t$, could be caused by reciprocating masses, unbalanced rotors with constant angular velocities, or rotor with time-dependent spin rates.

2 Satellite Model

The model used in this study is a torque-free, quasi-rigid body that is perturbed by time-dependent subbody motion. The quasi-rigid-body approximation is often used as a tool to study complex spacecraft systems and obtain analytical information about their global behavior. Understanding these rigid-body approximations is often the first step in a complete study of a complex spacecraft. The damping, which is implied by the term "quasi-rigid," is modeled by a quantitative energy sink technique recently derived by Kammer and Gray (1992).

The specific spacecraft model used in this investigation is shown in Fig. 1. The system's mass center c does not move relative to the carrier body since the two subbodies oscillate symmetrically with respect to c along the x-axis. The position of the subbodies relative to the carrier is a known periodic function of time and is denoted by $\eta(t)$. The $\eta = 0$ position is located a distance l from the mass center c. We let x, y, z denote a body-fixed orthogonal coordinate system aligned with the principal axes of the carrier body and centered at c. The principal moments of inertia of the carrier with respect to c are designated I_1, I_2, I_3. The moments of inertia are distinct and we assume $I_1 < I_2 < I_3$.

In order to apply Melnikov's method, it is assumed that the subbodies of mass m are "small" in comparison to the main body. In addition, the damping is assumed to be small. What we mean by small will be defined later with respect to a perturbation parameter ϵ. Therefore, both the subbodies and the damping mechanism are assumed to have an $\mathcal{O}(\epsilon)$ perturbing effect on the spacecraft.

3 Equations of Motion

Using standard methods such as Lagrange's equations or Newton-Euler techniques, the undamped equations of motion can be derived in terms of principal, body angular momentum components h_1, h_2, h_3 as

$$\dot{h}_1 = \left[\frac{B - C}{(B + \Delta)(C + \Delta)}\right] h_2 h_3 \tag{1}$$

$$\dot{h}_2 = \left(\frac{1}{A} - \frac{1}{C + \Delta}\right) h_1 h_3 \tag{2}$$

$$\dot{h}_3 = \left(\frac{1}{B + \Delta} - \frac{1}{A}\right) h_1 h_3 \tag{3}$$

where $A \triangleq I_1$, $B \triangleq I_2 + 2ml^2$, $C \triangleq I_3 + 2ml^2$, $\Delta = \Delta(t) \triangleq 2m\eta(t)[2l + \eta(t)]$, and the dot $(\dot{})$ denotes differentiation with respect to time, $d()/dt$.

The damping terms modeling the quasi-rigid body are readily added via the argument presented in Kammer and Gray (1992). The damping is implemented via a nonlinear control design that quantitatively simulates the effects of internal damping mechanisms which can be accurately modeled as energy sinks. The controller dissipates kinetic energy while maintaining the magnitude of the angular momentum vector. The control torques are nonlinear functions of the angular momentum components expressed in the body-fixed frame. Kammer and Gray (1992) specify a control law by identifying the conditions which must be met by the controller to simulate onboard energy dissipation. Assuming an asymmetric rigid-body representation for a spacecraft with principal mass moments of inertia $I_1 < I_2 < I_3$, Euler's equations for the attitude motion in momentum space are given by

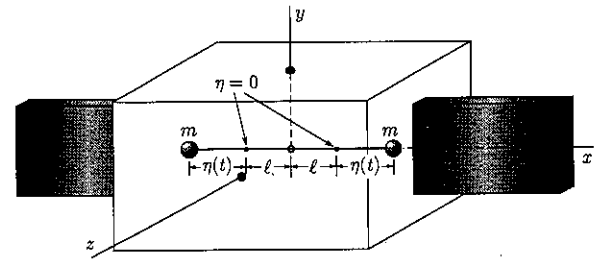

Fig. 1 The model spacecraft configuration

$$\dot{h}_1 = \frac{I_2 - I_3}{I_2 I_3} h_2 h_3 + u_1$$

$$\dot{h}_2 = \frac{I_3 - I_1}{I_1 I_3} h_1 h_3 + u_2$$

$$\dot{h}_3 = \frac{I_1 - I_2}{I_1 I_2} h_1 h_2 + u_3 \tag{4}$$

where the h_i are the components of the angular momentum vector $\mathbf{H}$ measured along the body-fixed principal axes and the u_i are the control torques which are nonlinear functions of the h_i to be determined.

The conditions that the controller must satisfy are that the magnitude of the angular momentum vector $\mathbf{H}$ must be conserved, the time derivative of the system kinetic energy must be negative semi-definite, and the controller must not dissipate energy for a pure spin about any of the principal axes. Although these conditions do not uniquely determine the form of the control law, for the purpose of energy sink simulation, we choose the control design given by

$$u_1 = -\beta h_1 h_2^2$$

$$u_2 = \beta h_2 \left(h_1^2 - h_3^2\right)$$

$$u_3 = \beta h_3 h_2^2 \tag{5}$$

where β is a positive valued control gain to be specified.

It can be shown that the control law given by Eq. (5) satisfies the above three conditions and that the closed loop equations of motion possess the same topological structure as the equations for a damped single-body spacecraft.

The equations of motion in Eqs. (1)–(3) become

$$\dot{h}_1 = \left[\frac{B - C}{(B + \Delta)(C + \Delta)}\right] h_2 h_3 - \beta h_1 h_2^2, \tag{6}$$

$$\dot{h}_2 = \left(\frac{1}{A} - \frac{1}{C + \Delta}\right) h_1 h_3 + \beta h_2 \left(h_1^2 - h_3^2\right), \tag{7}$$

$$\dot{h}_3 = \left(\frac{1}{B + \Delta} - \frac{1}{A}\right) h_1 h_2 + \beta h_2^2 h_3. \tag{8}$$

It is clear that Δ is the term that makes the system nonautonomous since $\Delta = \Delta(\eta)$ and η is a specified function of time.

We now nondimensionalize Eqs. (6)–(8). In order to perform the transformation, we define the following scaled quantities:

$$\epsilon \triangleq ml^2/B \qquad \tilde{h}_i \triangleq h_i/H \qquad \tilde{h}'_i \triangleq \frac{B}{H^2}\dot{h}_i$$

$$\tilde{\Delta} \triangleq \frac{\Delta}{\epsilon B} \qquad \tilde{\beta} \triangleq \beta\frac{HB^2}{ml^2} \qquad \tau \triangleq Ht/B$$

$$r_1 \triangleq C/B \qquad r_2 \triangleq A/B$$

where H is the total angular momentum and differentiation with respect to nondimensional time τ is denoted by a prime, $()' = d()/d\tau$. All quantities except ϵ are $\mathcal{O}(1)$. Notice that the number of moment of inertia parameters has been reduced to two, r_1 and r_2. The size of the parameter region involving the moments of inertia is now restricted to an easily determined domain due to the assumptions made on their relative size and the natural physical limitations restricting the choice of moments of inertia. We have assumed that $I_1 < I_2 < I_3$, therefore $A < B < C$. It immediately follows that $0 < r_2 < 1 < r_1$. In addition, since it can be shown that the individual moments of inertia are interrelated by $A + B > C$, it follows that $r_2 + 1 > r_1$ and therefore

$$0 < r_2 < 1 < r_1 < 1 + r_2. \tag{9}$$

These inequalities will restrict the size of the parameter space involving r_1 and r_2 that needs to be studied.

We do not use the usual Smelt (often called DeBra-Delp, see Rimrott, 1989) parameters since they were originally defined to simplify equations of motion when written in terms of angular velocity components, not angular momentum components. Our equations are much simpler when using the definitions for r_1 and r_2 given above. The final results will also be written in terms of the Smelt parameters so that the results can be shown in more familiar terms. Carrying out the above change of variables leads to an equivalent set of dimensionless equations:

$$\tilde{h}'_1 = \frac{1 - r_1}{(1 + \epsilon\tilde{\Delta})(r_1 + \epsilon\tilde{\Delta})}\tilde{h}_2\tilde{h}_3 - \epsilon\tilde{\beta}\tilde{h}_1\tilde{h}_2^2, \tag{10}$$

$$\tilde{h}'_2 = \left(\frac{1}{r_2} - \frac{1}{r_1 + \epsilon\tilde{\Delta}}\right)\tilde{h}_1\tilde{h}_3 + \epsilon\tilde{\beta}\tilde{h}_2\left(\tilde{h}_1^2 - \tilde{h}_3^2\right), \tag{11}$$

$$\tilde{h}'_3 = \left(\frac{1}{1 + \epsilon\tilde{\Delta}} - \frac{1}{r_2}\right)\tilde{h}_1\tilde{h}_2 + \epsilon\tilde{\beta}\tilde{h}_2^2\tilde{h}_3. \tag{12}$$

Equations (10)–(12) are the full nondimensional equations of motion explicitly containing the perturbation parameter ϵ. No assumptions have yet been made about the size of any of the quantities in the development of the equations, although the definitions of the nondimensional quantities and ϵ are convenient for assumptions made later.

4 The Unperturbed Phase Space

In order to apply Melnikov's method to the system of Eqs. (10)–(12), there must be a heteroclinic cycle in the unperturbed phase space, and the unperturbed system must be integrable. The solution to the unperturbed system is needed since Melnikov's method makes use of the globally computable solutions of the unperturbed *integrable* system in computing the perturbed solutions. It can be shown that the attitude dynamics of a torque-free rigid body, when measured in body angular momentum components, occur on the surface of the angular momentum sphere (see Fig. 2). This sphere is also the reduced phase space for Euler's equations of motion for a torque-free rigid body. These equations are given by

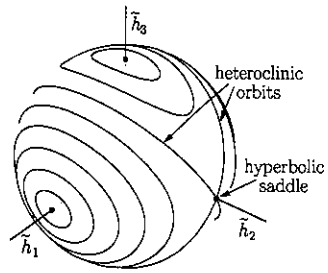

Fig. 2 The momentum sphere illustrating the heteroclinic orbits and the hyperbolic saddle points. The curves are orbits of constant energy.

$$\tilde{h}'_1 = \frac{1 - r_1}{r_1}\tilde{h}_2\tilde{h}_3, \tag{13}$$

$$\tilde{h}'_2 = \left(\frac{r_1 - r_2}{r_1 r_2}\right)\tilde{h}_1\tilde{h}_3, \tag{14}$$

$$\tilde{h}'_3 = \left(\frac{r_2 - 1}{r_2}\right)\tilde{h}_1\tilde{h}_2. \tag{15}$$

Equations (13)–(15) are just the equations of motion, Eqs. (10)–(12), with $\epsilon = 0$, i.e., the unperturbed equations of motion. Euler's equations are integrable in terms of Jacobi elliptic functions or hyperbolic functions, depending on the angular momentum and energy. The phase space is a two-dimensional surface imbedded in $\mathbb{R}^3$. This phase space possesses six fixed points or equilibria corresponding to positive and negative spin about each of the three principal axes of the satellite. Two of the fixed points, corresponding to spin about the intermediate principal axis, are hyperbolic fixed points or saddles. In addition, there are four heteroclinic orbits linking the hyperbolic fixed points as shown in Fig. 2. During the transition of an energy dissipating satellite from spin near the minimum moment of inertia axis to spin about the maximum moment of inertia axis, the trajectory must cross the heteroclinic orbits in the phase space. More precisely, the trajectory of the damped system must cross a heteroclinic orbit of the undamped system. We study the chaotic motion in the perturbed system that may occur near the heteroclinic orbits.

5 Melnikov's Method and Equation Transformation

Melnikov's method is applied to detect chaos in the system of Eqs. (10)–(12). For a detailed exposition of Melnikov theory, see Guckenheimer and Holmes (1983) and Wiggins (1990). Briefly, Melnikov's method is a perturbation technique for proving the existence of transverse heteroclinic[2] orbits to hyperbolic periodic orbits in a class of time-periodic vector fields. Though it is perturbation method, Melnikov's method gives *global* information about the system's dynamics. The essential idea in Melnikov's method is to use the globally computable solutions to the unperturbed *integrable* system in studying the perturbed solution. The existence of transverse heteroclinic orbits implies the existence of horseshoes and chaos via the Smale-Birkhoff Theorem. These horseshoes appear near the unperturbed heteroclinic orbit in a "chaotic layer." A typical trajectory, when going from minor axis to major axis spin, must go through this chaotic layer, and possibly near the horseshoe. Although horseshoes are not attractors, their existence has profound consequences for physically realizable motions. The orbits in the horseshoes are saddle-type hyperbolic and a nearby orbit can first be

[2]The method applies equally well to systems with homoclinic orbits.

attracted to the chaotic horseshoe orbits and then be repelled from them. Therefore, when horseshoes are present, it is possible to see long chaotic transients before orbits settle down to equilibria or periodic orbits, see Greenspan and Holmes (1983), Guckenheimer and Holmes (1983), and Palis and Takens (1993).

However, the phase space, and in particular the chaotic layer, is very complex. Numerical and theoretical work on Duffing's equation suggests that stable subharmonic motions are possible, although the stable subharmonics of high period in the chaotic layer are thought to be unobservable. This is because the basins of attraction of the high period subharmonics are so small that numerical or physical noise dominates and perturbs the orbit out of a basin, making the orbit appear like transient chaos. Numerical work on Duffing's equations also shows "strange attractor" chaos for moderate values of damping and forcing, but the strange attractor does not coexist with stable T-periodic orbits. Since the stable T-periodic orbits correspond to slightly perturbed major axis spin in the satellite equations, this suggests that a chaotic attractor might not occur for parameter ranges of interest when studying the satellite attitude transition maneuver. Here we are assuming that it is reasonable to study the attitude transition to major axis spin only when the satellite design has already ensured that the final major axis spin dynamics are a simple periodic orbit. For a detailed discussion of all of these issues, see Greenspan and Holmes (1983) and Guckenheimer and Holmes (1983).

We are now left with the tasks of solving for the heteroclinic orbit $\mathbf{q}_0(t)$ of the unperturbed system, writing the perturbed equations of motion such that only terms through $\mathcal{O}(\epsilon)$ are kept, and then obtaining the two independent equations of motion (in convenient coordinates) describing the dynamics on the surface of the momentum sphere.

5.1 Solution for the Unperturbed Heteroclinic Orbit $q_0(t)$. For a torque-free rigid body with equations of motion given by Eqs. (13)–(15), there are two integrals of the motion—momentum and energy. In nondimensional coordinates, these integrals are given by

$$\tilde{h}_1^2 + \tilde{h}_2^2 + \tilde{h}_3^2 = 1 \qquad \text{(momentum)} \tag{16}$$

$$\frac{\tilde{h}_1^2}{r_2} + \tilde{h}_2^2 + \frac{\tilde{h}_3^2}{r_1} = \tilde{T} \quad \text{(energy)} \tag{17}$$

where $\tilde{T} \triangleq 2BT/H^2$ is the nondimensional total energy and T is the total energy. Any trajectory on the momentum sphere is determined by the intersection of the momentum sphere $\mathcal{S}$ defined by Eq. (16) and the energy ellipsoid $\mathcal{E}$ defined by Eq. (17). Recall that when viewed in body coordinates, the angular momentum vector appears to move such that its tip always remains on a particular intersection of $\mathcal{S}$ and $\mathcal{E}$. The radius of $\mathcal{S}$, which is $\tilde{H} = 1$, must lie between the smallest and largest semiaxes of the ellipsoid. Since $A < B < C$, or nondimensionally $0 < r_2 < 1 < r_1$, the condition on the radius of $\mathcal{S}$ is given by $r_2\tilde{T} < 1 < r_1\tilde{T}$. Since the heteroclinic orbits are formed when the $\mathcal{S}$ and $\mathcal{E}$ surfaces are tangent at the points $(0, \pm 1, 0)$, the energy level for the heteroclinic orbits must be given by $T = H^2/(2B)$, or $\tilde{T} = 1$ in terms of our nondimensional parameterization. The energy integral then becomes

$$\frac{\tilde{h}_1^2}{r_2} + \tilde{h}_2^2 + \frac{\tilde{h}_3^2}{r_1} = 1. \tag{18}$$

Using Eqs. (13), (14), (15), (16), and (18), it can be shown that the solutions for the $\tilde{h}_i$ along the heteroclinic orbits are given by (Hughes, 1986)

$$\tilde{h}_{1u} = \pm\left[\frac{r_2(1-r_1)}{r_2-r_1}\right]^{1/2} \operatorname{sech}\left\{\left[\frac{(r_2-1)(1-r_1)}{r_1 r_2}\right]^{1/2}\tau\right\} \tag{19}$$

$$\tilde{h}_{2u} = \pm\tanh\left\{\left[\frac{(r_2-1)(1-r_1)}{r_1 r_2}\right]^{1/2}\tau\right\} \tag{20}$$

$$\tilde{h}_{3u} = \pm\left[\frac{r_1(r_2-1)}{r_2-r_1}\right]^{1/2} \operatorname{sech}\left\{\left[\frac{(r_2-1)(1-r_1)}{r_1 r_2}\right]^{1/2}\tau\right\} \tag{21}$$

where the subscript u signifies an unperturbed quantity, $\tau = 0$ has been chosen to eliminate constants of integration, and the appropriate signs are chosen to give the four heteroclinic trajectories.

5.2 Equations of Motion to $\mathcal{O}(\epsilon)$. Using binomial expansions, the equations of motion given by Eqs. (10)–(12) can be expressed as

$$\tilde{h}_1' = \left(\frac{1-r_1}{r_1}\right)\tilde{h}_2\tilde{h}_3 - \epsilon\left[\left(\frac{1-r_1^2}{r_1^2}\right)\tilde{\Delta}\tilde{h}_2\tilde{h}_3 + \tilde{\beta}\tilde{h}_1\tilde{h}_2^2\right] \tag{22}$$

$$\tilde{h}_2' = \left(\frac{r_1-r_2}{r_1 r_2}\right)\tilde{h}_1\tilde{h}_3 + \epsilon\left[\frac{\tilde{\Delta}}{r_1^2}\tilde{h}_1\tilde{h}_3 + \tilde{\beta}\tilde{h}_2\left(\tilde{h}_1^2 - \tilde{h}_3^2\right)\right] \tag{23}$$

$$\tilde{h}_3' = \left(\frac{r_2-1}{r_2}\right)\tilde{h}_1\tilde{h}_2 + \epsilon\left(\tilde{\beta}\tilde{h}_2^2\tilde{h}_3 - \tilde{\Delta}\tilde{h}_1\tilde{h}_2\right) \tag{24}$$

where only terms through $\mathcal{O}(\epsilon)$ have been retained.

We now transform to spherical coordinates. It is convenient to choose the coordinate transformation so that one of the new coordinates is zero along the unperturbed trajectory. This can easily be done since the heteroclinic orbits are great circles on the momentum sphere. Consider the heteroclinic orbit that lies in the region $\tilde{h}_1 > 0$ and $\tilde{h}_3 > 0$. The angle ν between the $\tilde{h}_1$–$\tilde{h}_2$ plane and this heteroclinic orbit can be shown to be

$$\nu = \arctan\left[\frac{r_1(r_2-1)}{r_2(1-r_1)}\right]^{1/2}. \tag{25}$$

Starting with a set of coordinates ξ_1, ξ_2, ξ_3 aligned with the $\tilde{h}_1$, $\tilde{h}_2$, $\tilde{h}_3$ system, rotate the ξ coordinate system through the angle $-\nu$ about the $\tilde{h}_2$-axis so that the positive ξ_1-axis pierces the heteroclinic orbit in the region $\tilde{h}_1 > 0$, $\tilde{h}_3 > 0$. We can then transform from the ξ coordinates to the dimensionless spherical coordinates ϕ and θ to obtain the following equations relating the $\tilde{h}_i$, and ν, θ, and ϕ:

$$\tilde{h}_1 = \cos\nu\cos\theta\cos\phi - \sin\nu\sin\phi, \tag{26}$$

$$\tilde{h}_2 = \sin\theta\cos\phi, \tag{27}$$

$$\tilde{h}_3 = \sin\nu\cos\theta\cos\phi - \cos\nu\sin\phi. \tag{28}$$

Note that there is no radial dependence since the angular momentum sphere has a constant radius. The derivatives with respect to τ are also needed and they are given by

$$\tilde{h}_1' = \phi'(-\cos\nu\sin\phi\cos\theta - \sin\nu\cos\phi) - \theta'\cos\nu\sin\theta\cos\phi, \tag{29}$$

$$\tilde{h}_2' = \theta'\cos\theta\cos\phi - \phi'\sin\theta\sin\phi, \tag{30}$$

$$\tilde{h}_3' = \phi'(\cos\nu\cos\phi - \sin\nu\cos\theta\sin\phi) - \theta'\sin\nu\sin\theta\cos\phi. \tag{31}$$

Equations (26)–(31) are then substituted into Eqs. (22)–(24) and *any* two of the resulting three equations are then solved, using computer algebra (Wolfram, 1991), for θ' and ϕ'. Note that only two of the equations are independent due to the fact that our phase space lies on the surface of the sphere and is therefore two dimensional. This gives the final two first-order differential equations to which Melnikov's method is applied

$$\begin{aligned}\phi' = &\{[(r_2 - r_1)c\nu c2\nu + r_2(r_1 - 1)c\nu]c\phi c\theta s\phi s\theta \\ &+ [(r_2 - r_1)c^2\nu s\nu + r_2(r_1 - 1)s\nu]c^2\phi c^2\theta s\theta \\ &+ (r_1 - r_2)c^2\nu s\nu s^2\phi s\theta\}/r_1r_2(s\nu c\phi c\theta + c\nu s\phi) \\ &+ \epsilon\{\tilde{\Delta}[(2c\nu s^2\nu - r_1^2c\nu)c\phi c\theta s\phi s\theta \\ &+ (s^3\nu - r_1^2s\nu)c^2\phi c^2\theta s\theta + c^2\nu s\nu s^2\phi s\theta] \\ &+ \tilde{\beta}[r_1^2s\nu(4c^2\nu - 1)c^2\phi c\theta s\phi s^2\theta + 2r_1^2c\nu s^2\phi c^3\phi c^2\theta s^2\theta \\ &+ r_1^2c\nu c2\nu c\phi s^2\phi s^2\theta]\}/r_1^2(s\nu c\phi c\theta + c\nu s\phi). \quad (32)\end{aligned}$$

and

$$\begin{aligned}\theta' = &\{(r_1 - r_2)[c\nu s^2\nu c^3\phi c^2\theta + s\nu c2\nu c^2\phi c\theta s\phi \\ &+ c^2\nu s\nu c^2\phi c^3\theta s\phi - c\nu s^2\nu c\phi s^2\phi + c\nu c2\nu c\phi c^2\theta s^2\phi \\ &- c^2\nu s\nu c\theta c^3\phi] + r_2(r_1 - 1)[s\nu c^2\phi c\theta s\phi s^2\theta \\ &+ c\nu c\phi s^2\phi s^2\theta]\}/r_1r_2(s\nu c^2\phi c\theta + c\nu c\phi s\phi) \\ &+ \epsilon\{\tilde{\Delta}[c\nu s^2\nu c^3\phi c^2\theta + s\nu c2\nu c^2\phi c\theta s\phi + c^2\nu s\nu c^2\phi c^3\theta s\phi \\ &- c\nu s^2\nu c\phi s^2\phi + c\nu c2\nu c\phi c^2\theta s^2\phi - c^2\nu s\nu c\theta s^3 \\ &+ (1 - r_1^2)(s\nu c^2\phi c\theta s\phi s^2\theta + c\nu c\phi s^2\phi s^2\theta)] \\ &+ \tilde{\beta}[r_1^2s\nu c2\nu c^4\phi c^2\theta s\theta - 4r_1^2c\nu s^2\nu c^3\phi c\theta s\phi s\theta \\ &+ r_1^2c\nu c2\nu c^3\phi c^3\theta s\phi s\theta - r_1^2s\nu c2\nu c^2\phi s^2\phi s\theta \\ &- 4r_1^2c^2\nu s\nu c^2\phi c^2\theta s^2\phi s\theta \\ &- r_1^2c\nu c2\nu c\phi c\theta s^3\phi s\theta \\ &+ r_1^2c\nu c^3\phi c\theta s\phi s^3\theta - r_1^2s\nu c^2\phi s^2\phi s^3\theta]\} \\ &/r_1^2(s\nu c^2\phi c\theta + c\nu c\phi s\phi), \quad (33)\end{aligned}$$

where

$$s \triangleq \sin \text{ and } c \triangleq \cos. \quad (34)$$

Equations (32) and (33) are in the desired form, $\phi' = f_1 + \epsilon g_1$ and $\theta' = f_2 + \epsilon g_2$ (see the following section). Finally, the unperturbed solutions given by Eqs. (19)–(21) must be transformed to the same set of spherical coordinates. This transformation gives

$$\sin\theta_u = -\tanh\left\{\left[\frac{(r_2 - 1)(1 - r_1)}{r_1r_2}\right]^{1/2}\tau\right\} \quad (35)$$

$$\cos\theta_u = \operatorname{sech}\left\{\left[\frac{(r_2 - 1)(1 - r_1)}{r_1r_2}\right]^{1/2}\tau\right\} \quad (36)$$

$$\phi_u = 0 \quad (37)$$

along the selected unperturbed heteroclinic orbit, and time was chosen to move along the trajectory from positive to negative $\tilde{h}_2$.

6 The Melnikov Function

Melnikov's method considers systems of the form

$$\dot{\mathbf{x}} = \mathbf{f}(\mathbf{x}) + \epsilon\mathbf{g}(\mathbf{x},t), \quad \mathbf{x} = \begin{Bmatrix} u \\ v \end{Bmatrix} \in \mathbb{R}^2 \quad (38)$$

where $\mathbf{g}$ is of period T in t, $\mathbf{f}(\mathbf{x})$ is a Hamiltonian vector field defined on $\mathbb{R}^2$ and $\epsilon\mathbf{g}(\mathbf{x}, t)$ is a small perturbation which is not necessarily Hamiltonian.

We define the Melnikov function

$$M(t_0) = \int_{-\infty}^{\infty} \mathbf{f}(\mathbf{q}_0(t)) \wedge \mathbf{g}(\mathbf{q}_0(t), t + t_0)\,dt \quad (39)$$

where the symbol $\wedge$ is the wedge operator, defined by $\mathbf{a} \wedge \mathbf{b} = a_1b_2 - a_2b_1$.

Referring to Eqs. (38), (32), and (33), we can easily identify the components of the vector functions $\mathbf{f} = (f_1, f_2)$ and $\mathbf{g} = (g_1, g_2)$ for use in the Melnikov integral, Eq. (39). We must now prescribe the time-dependent form of η by letting $\tilde{\eta} \triangleq \eta/l$, $\tilde{\Omega} \triangleq \Omega B/H$, and $\eta \triangleq \eta_0 \cos(\Omega t)$. This definition corresponds to a simple periodic oscillation of the masses, thus modeling phenomena such as reciprocating masses, unbalanced rotors with constant angular velocities, or rotors with time-dependent spin rates.

Any time-dependent form may be chosen for η, but it is clear that some are more tractable than others, and the periodic form we choose accurately models the phenomena we have discussed. It follows that the nondimensional form of Δ is then

$$\tilde{\Delta} = \tilde{\eta}^2 + 4\tilde{\eta}\cos(\tilde{\Omega}\tau) + \tilde{\eta}^2\cos(2\tilde{\Omega}\tau). \quad (40)$$

Substituting the unperturbed solutions $\mathbf{q}_0(\tau)$, given by Eqs. (35)–(37), into $\mathbf{f}(\mathbf{q}_0(\tau))$ and $\mathbf{g}(\mathbf{q}_0(\tau), \tau + \tau_0)$, carrying out the wedge product, and substituting the result into the Melnikov integral given by Eq. (39) yields

$$\begin{aligned}M(\tau_0) = \int_{-\infty}^{\infty} &[-C_1C_3\tilde{\eta}^2\operatorname{sech}^2(C_1\tau)\tanh(C_1\tau) \\ &- 4C_1C_3\tilde{\eta}\cos\left(\tilde{\Omega}(\tau + \tau_0)\right)\operatorname{sech}^2(C_1\tau)\tanh(C_1\tau) \\ &- C_1C_3\tilde{\eta}^2\cos\left(2\tilde{\Omega}(\tau + \tau_0)\right)\operatorname{sech}^2(C_1\tau)\tanh(C_1\tau) \\ &+ C_4\bar{\beta}\operatorname{sech}^2(C_1\tau)\tanh^2(C_1\tau)]\,d\tau. \quad (41)\end{aligned}$$

where the following new quantities have been defined:

$$C_1 \triangleq \left[\frac{(r_1 - 1)(1 - r_2)}{r_1r_2}\right]^{1/2} = C_1(r_1,r_2), \quad (42)$$

$$C_3 \triangleq \frac{(r_1 - 1)(r_2 - r_1 - 1)}{r_1(r_2 - r_1)} = C_3(r_1,r_2), \quad (43)$$

$$C_4 \triangleq \frac{2(r_1 - 1)(r_2 - 1)}{r_2 - r_1} = C_4(r_1,r_2). \quad (44)$$

The evaluation of the integrals in Eq. (41) can be accomplished via the residue theorem of complex variable theory. Upon carrying out the integration, we obtain the following Melnikov function:

$$\begin{aligned}M(\tau_0) = &\frac{2C_4\tilde{\beta}}{3C_1} + \frac{2\pi C_3\tilde{\eta}\tilde{\Omega}^2}{C_1^2} \\ &\times\left[\frac{\sin\left(\tilde{\Omega}\tau_0\right)}{\sinh\left[\pi\tilde{\Omega}/(2C_1)\right]} + \tilde{\eta}\frac{\sin\left(2\tilde{\Omega}\tau_0\right)}{\sinh\left(\pi\tilde{\Omega}/C_1\right)}\right]. \quad (45)\end{aligned}$$

Melnikov theory states that the condition for chaos is that $M(\tau_0)$ change sign for some τ_0. Inspection of the Melnikov function reveals that there are two harmonic terms, one with

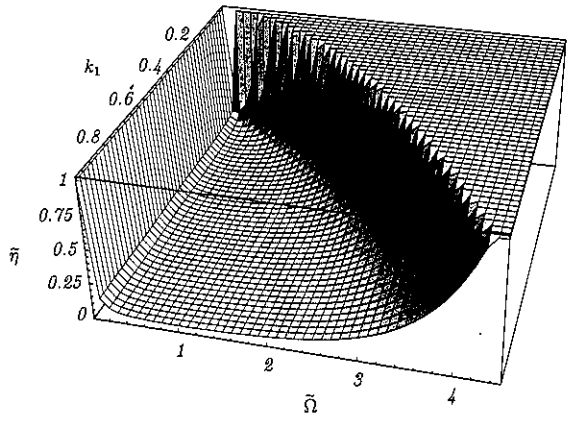

Fig. 3 The surface separating chaotic from nonchaotic motion for the parameter space $\tilde{\Omega}$-$\tilde{\eta}$-k_1 as given by the Melnikov criterion in Eq. (49). The parameters $\tilde{\beta}$ and k_3 were chosen to have the values 0.1 and 2/3, respectively.

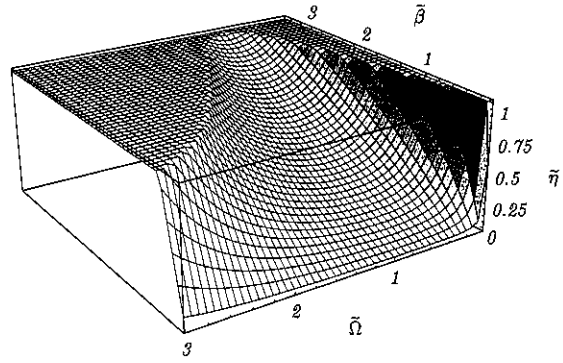

Fig. 4 The surface separating chaotic from nonchaotic motion for the parameter space $\tilde{\Omega}$-$\tilde{\eta}$-$\tilde{\beta}$ as given by the Melnikov criterion in Eq. (47). The parameters k_1 and k_3 were chosen to have the values 0.8 and 2/3, respectively.

twice the frequency of the other. Therefore, the maximum amplitude of the factor containing the harmonic terms is some function $F_{\max}$ of *both* of the harmonic amplitudes. It can be shown that $F_{\max}$ is given by

$$F_{\max} = \frac{1}{4}\left(3\mathfrak{A} + \sqrt{\mathfrak{A}^2 + 32\,\mathfrak{B}^2}\right) \times \left[\frac{1}{2} + \frac{\mathfrak{A}}{32\,\mathfrak{B}^2}\left(\sqrt{\mathfrak{A}^2 + 32\,\mathfrak{B}^2} - \mathfrak{A}\right)\right]^{1/2}, \quad (46)$$

Given this relationship for $F_{\max}$, the criterion for chaos becomes

$$\frac{3\pi(r_2 - r_1 - 1)\sqrt{r_2}\,\tilde{\eta}\tilde{\Omega}^2 F_{\max}}{2(r_2 - 1)\sqrt{r_1(r_1 - 1)(1 - r_2)}} > \tilde{\beta}. \quad (47)$$

Equation (47) gives the analytical condition for chaos. This result divides the parameter space into regions where horseshoes and chaotic transients exist from regions where they do not. Close inspection reveals that Eq. (47) is a function of the five system parameters, r_1, r_2, $\tilde{\eta}$, $\tilde{\Omega}$, and $\tilde{\beta}$. If Eq. (47) is satisfied, then the system modeled by Eqs. (10)–(12) exhibits chaotic dynamics near the heteroclinic orbits for sufficiently small ϵ.

Before discussing the analytical Melnikov result, we first write Eq. (47) in terms of the Smelt (DeBra-Delp) parameters so that it can also be interpreted within that framework. Various authors define the Smelt parameters differently, but here we use the same definitions that DeBra and Delp (1961) used in their original paper

$$k_1 \triangleq \frac{C - B}{A}, \quad k_2 \triangleq \frac{A - C}{B}, \quad k_3 \triangleq \frac{B - A}{C}.$$

Then, choosing to use k_1 and k_3 as the two moment of inertia parameters, r_1 and r_2 become

$$r_1 = \frac{1 + k_1}{1 + k_1 k_3}, \quad r_2 = \frac{1 - k_3}{1 + k_1 k_3}. \quad (48)$$

Since $A < B < C$, it can be shown (Rimrott, 1989) that $0 < k_1 < 1$ and $0 < k_3 < 1$.

Using the relations in Eqs. (48), the definition for $F_{\max}$ remains unchanged, but the definition for C_1 becomes

$$C_1 = \sqrt{k_1 k_3}$$

and, the expression in Eq. (47) of the criterion for chaos becomes

$$\frac{3\pi(1 + k_3)(1 + k_1 k_3)\tilde{\eta}\tilde{\Omega}^2 F_{\max}}{2k_3(1 + k_1)\sqrt{k_1 k_3}} > \tilde{\beta} \quad (49)$$

where $F_{\max}$ is given by Eq. (46).

7 Results

We have analytically proven the existence of transient chaos in the attitude motion of a quasi-rigid satellite with non-Hamiltonian, time-periodic perturbations. The derived criterion can be used to find chaotic and nonchaotic regions in parameter space and, if necessary, avoid chaotic motion in this class of satellite systems. The Melnikov criterion for chaos depends on five parameters: moment of inertia parameters r_1 and r_2 (or k_1 and k_3), forcing frequency $\tilde{\Omega}$, forcing amplitude $\tilde{\eta}$, and the damping $\tilde{\beta}$. By fixing two of the parameters, the others can be studied in a three-dimensional parameter space. Parametric studies of three-dimensional parameter subspaces for Eqs. (47) and (49) are shown in Figs. 3–6.

Figure 3 shows the dividing surface between chaotic and nonchaotic motion in $\tilde{\Omega}$-$\tilde{\eta}$-k_1 space as determined by Eq. (49). The moment of inertia parameter k_3 was chosen to be equal to 2/3 and the damping parameter $\tilde{\beta}$ was set equal to 0.1. By fixing $\tilde{\beta}$ at 0.1, we are not only fixing the amount of damping, but we are also fixing the size of the perturbing masses. Values of the parameters *above* the surface are chaotic. The surface "flattens" out at $\tilde{\eta} = 1$ since we impose $\tilde{\eta} < 1$ due to limits in the motion of the perturbing subbodies, i.e., we do not consider values of $\tilde{\eta} > 1$, corresponding to motion of the masses which pass through the spacecraft's mass center c. This is true for all figures where the surface flattens at $\tilde{\eta} = 1$. We can see that as k_1 increases it becomes easier to achieve chaotic motion. In addition we see what appears to be a resonance condition in the $\tilde{\Omega}$-$\tilde{\eta}$ plane. This resonance frequency changes slightly as k_1 changes and therefore depends on the shape of the satellite. The dependence of this resonance frequency upon the "natural" frequencies occurring in the motion of a torque-free rigid body, such as precessional and nutational frequencies, is being investigated. For small and large values of $\tilde{\Omega}$, it is impossible to obtain chaos for any value of $\tilde{\eta} < 1$. Whereas for intermediate values of $\tilde{\Omega}$ (e.g., $\tilde{\Omega} \approx 0.25$–$0.35$), chaos is much easier to attain and is virtually assured for large values of $k_1 \to 1$. We also see that for values of k_1 approaching zero, which corresponds to a nearly symmetric, prolate rigid body, no chaotic motion occurs for the constant values of k_3 and $\tilde{\beta}$ chosen and for $\tilde{\eta} < 1$ and *any* values of $\tilde{\Omega}$ and k_1.

Figure 4 illustrates the dividing surface between chaotic and nonchaotic regions in $\tilde{\Omega}$-$\tilde{\eta}$-$\tilde{\beta}$ space as determined by Eq.

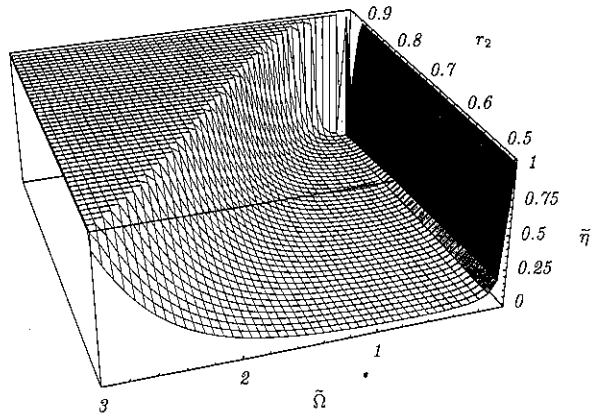

Fig. 5 The surface separating chaotic from nonchaotic motion for the parameter space $\tilde{\Omega}$-$\tilde{\eta}$-r_2 as given by the Melnikov criterion in Eq. (47). The parameters $\tilde{\beta}$ and r_1 were chosen to have the values 0.1 and 1.5, respectively.

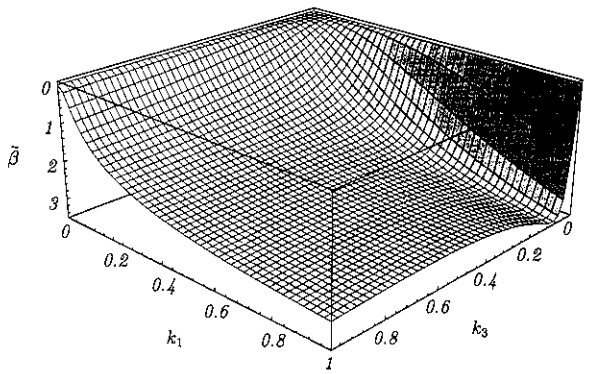

Fig. 6 The surface separating chaotic from nonchaotic motion for the parameter space $\tilde{\beta}$-k_1-k_3 as given by the Melnikov criterion in Eq. (49). The parameters $\tilde{\eta}$ and $\tilde{\Omega}$ were chosen to have the values 0.9 and 0.5, respectively.

(47). As in Fig. 3, the chaotic region is above the surface. We again see the resonance effect in the $\tilde{\Omega}$-$\tilde{\eta}$ plane, but now at $\tilde{\Omega} \approx 0.5$. The resonance frequency is constant in this figure since the moments of inertia of the satellite (k_1 and k_3) are fixed for all values of $\tilde{\eta}$, $\tilde{\Omega}$, and $\tilde{\beta}$ and therefore the shape of the satellite does not vary. As $\tilde{\beta} \to 0$, chaotic motion occurs for all values of $\tilde{\Omega}$ and $\tilde{\eta}$, which is what we expect from the theory of Hamiltonian systems: a generic perturbation of a Hamiltonian system yields chaotic motion in a layer surrounding a heteroclinic orbit (Lichtenberg and Lieberman, 1992). In addition, we see that if $\tilde{\beta}$ is increased to large enough values, it is impossible to attain chaotic motion for values of $\tilde{\eta} < 1$. This too is physically reasonable: sufficient damping suppresses the chaos. We should also note that $\tilde{\beta} \propto 1/m$, where m is the perturbing mass. Thus, as m is increased, $\tilde{\beta}$ decreases and we find that the chaotic surface is more easily reached. This too agrees with intuition. Larger perturbations (i.e., oscillating masses) are more likely to produce chaotic motion. If the masses are made small enough for a fixed amount of satellite damping, they will have a negligible effect on the satellite and chaotic motion will be impossible.

Figure 5 shows the dividing surface between chaotic and nonchaotic motion in $\tilde{\Omega}$-$\tilde{\eta}$-r_2 space for $\tilde{\beta} = 0.1$ and $r_1 = 3/2$. Motion is chaotic for values above the surface. The parameter r_2 ranges from 0.5 to 1 since r_1 was chosen to be 1.5 (see Eq. (9)). The behavior is very interesting in that chaotic motion is virtually assured for values of r_2 approaching unity and small values of $\tilde{\Omega}$. This corresponds to a nearly symmetric oblate spacecraft with small perturbing frequencies. This supplements the result described above for a nearly symmetric prolate spacecraft where chaos is impossible to attain. These results are not obvious and are a subject for further study.

In Fig. 6 the chaotic region is above the surface shown. It can be seen that for smaller values of k_3 and larger values of k_1, chaos can be achieved for a range of $\tilde{\beta}$. On the other hand, as $k_1 \to 0$ and $k_3 \to 1$, chaos cannot be achieved no matter how small $\tilde{\beta}$ is made. Again, $k_1 \to 0$ corresponds to a nearly symmetric and prolate body, and it is impossible to have chaos. As $k_3 \to 0$ the body becomes nearly symmetric and oblate and chaotic motion is assured for a large range of $\tilde{\beta}$.

It is important to note that the results correspond specifically to the case where the oscillating masses are aligned with the minor principal axis.

8 Conclusion

We have derived an analytical criterion for the occurrence of a chaotic region of phase space in terms of system parameters for an energy dissipating, quasi-rigid satellite with time-periodic perturbations. The analytical criterion for the occurrence of chaos is obtained by applying Melnikov's method to a quasi-rigid satellite model. This model is a Hamiltonian system perturbed by a non-Hamiltonian perturbation in the form of oscillations of subbodies and damping in the satellite. It is obvious from the modern theory of nonlinear dynamics that chaos can occur via the breakup of heteroclinic orbits in this class of systems. The contribution of this paper is the formulation of physically reasonable spacecraft models to which Melnikov's method can be applied and the performance of the difficult calculations required to obtain an uncomplicated criterion for chaos that can easily be used for satellite design.

The chaotic region occurs near heteroclinic orbits in the system's phase space and is traversed during a typical attitude maneuver. Since the chaotic region could introduce uncertainties into both the attitude maneuver and simulations checking the maneuver, it is prudent, at the present state of knowledge, to design the satellite so that the chaotic region does not exist. Chaos in the equations of motion for a satellite implies a sensitive dependence on initial conditions and a very complicated structure of the phase space. The sensitive dependence on initial conditions rules out the current practice of a straightforward check on the satellite attitude maneuver by a sample numerical integration. More extensive or elaborate simulations would have to be developed and applied to achieve confidence in a satellite design which maneuvered through a chaotic region. The specific effects of the chaotic region on the satellite mission are not well understood, but we suggest that the spacecraft could possibly be trapped in the chaotic layer for an unacceptably long time. The analytical criterion we have developed will be of great value in designing satellites such that chaotic motion is avoided.

In addition, subspaces of the full parameter space are readily studied to obtain a qualitative understanding of the interactions of the various parameters during chaotic motion. The complete Melnikov result is easily used to obtain the quantitative information needed when a satellite and its subsystems are being designed. Future work will further investigate this parameter space and extend our approach to better understand the onset of chaos in other classes of spacecraft.

Acknowledgments

The authors would like to thank Mark C. Stabb for his thoughtful discussions and assistance with the debugging of

Mathematica notebooks. The first author gratefully acknowledges the support of NASA through the National Space Grant College and Fellowship Program and the Wisconsin Space Grant Consortium. The second author gratefully acknowledges funding in part by NSF PYI grant ECS-9157192. In addition, the authors would like to acknowledge the work done by Junkins et al. (1973) as it was a major inspiration for our work.

References

Adams, G. J., 1980, "Dual-Spin Spacecraft Dynamics During Platform Spinup," *Journal of Guidance and Control*, Vol. 3, No. 1, pp. 29–36.

Baillieul, J., and Levi, M., 1987, "Rotational Elastic Dynamics," *Physica D.*, Vol. 27, pp. 43–62.

Barba, P. M., Furumoto, N., and Leliakov, I. P., 1973, "Techniques for Flat-Spin Recovery of Spinning Satellites," *AIAA Guidance and Control Conference*, Key Biscayne, FL, AIAA Paper 73-859.

Cochran, J. E., and Holloway, H. E., 1980, "Resonances in the Attitude Motions of Asymmetric Dual-Spin Spacecraft," *The Journal of the Astronautical Sciences*, Vol. 28, No. 3, pp. 231–254.

Cronin, D. L., 1978, "Flat Spin Recovery of a Rigid Asymmetric Spacecraft," *Journal of Guidance and Control*, Vol. 1, No. 4, pp. 281–282.

DeBra, D. B., and Delp, R. H., 1961, "Rigid Body Attitude Stability and Natural Frequencies in a Circular Orbit," *The Journal of the Astronautical Sciences*, Vol. 8, pp. 14–17.

Dovbysh, S. A., 1989, "Some New Dynamical Effects in the Perturbed Euler-Poinsot Problem Due to Splitting of Separatrices," *Journal of Applied Mathematics and Mechanics*, Vol. 53, No. 2, pp. 165–173.

Gebman, J. R., and Mingori, D. L., 1976, "Perturbation Solution for the Flat Spin Recovery of a Dual-Spin Spacecraft," *AIAA Journal*, Vol. 14, No. 7, pp. 859–867.

Greenspan, B. D., and Holmes, P. J., 1983, "Homoclinic Orbits, Subharmonics and Global Bifurcations in Forced Oscillations," *Nonlinear Dynamics and Turbulence*, G. I. Barenblatt, G. Iooss, and D. D. Joseph, eds., Pitman Publishing, Boston, MA, pp. 172–214.

Guckenheimer, J., and Holmes, P. J., 1983, *Nonlinear Oscillations, Dynamical Systems, and Bifurcations of Vector Fields*, Springer-Verlag, New York.

Hall, C. D., and Rand, R. H., 1991, "Spinup Dynamics of Axial Dual-Spin Spacecraft," *AAS/AIAA Astrodynamics Specialist Conference*, Durango, CO, Aug. 19–22, Paper AAS 91-403.

Holmes, P. J., and Marsden, J. E., 1983, "Horseshoes and Arnold Diffusion for Hamiltonian Systems on Lie Groups," *Indiana University Mathematics Journal*, Vol. 32, No. 2, pp. 273–309.

Hughes, P. C., 1986, *Spacecraft Attitude Dynamics*, John Wiley and Sons, New York.

Junkins, J. L., and Jacobson, I. D., and Blanton, J. N., 1973, "A Nonlinear Oscillator Analog of Rigid Body Dynamics," *Celestial Mechanics*, Vol. 7, pp. 398–407.

Kammer, D. C., and Gray, G. L., 1992, "A Nonlinear Control Design for Energy Sink Simulation in the Euler-Poinsot Problem," *The Journal of the Astronautical Sciences*, Vol. 41, No. 1, pp. 53–72.

Kaplan, M. H., and Cenker, R. J., 1973, "Control of Spin Ambiguity During Reorientation of an Energy Dissipating Body," *Journal of Spacecraft and Rockets*, Vol. 10, No. 12, pp. 757–760.

Koiller, J., 1984, "A Mechanical System with a 'Wild' Horseshoe," *Journal of Mathematical Physics*, Vol. 25, No. 5, pp. 1599–1604.

Krishnaprasad, P. S., 1985, "Lie-Poisson Structures, Dual-Spin Spacecraft and Asymptotic Stability," *Nonlinear Analysis, Theory, Methods & Applications*, Vol. 9, No. 10, pp. 1011–1035.

Krishnaprasad, P. S., and Marsden, J. E., 1987, "Hamiltonian Structures and Stability for Rigid Bodies with Flexible Attachments," *Archive for Rational Mechanics and Analysis*, Vol. 98, No. 1, pp. 71–93.

Lichtenberg, A. J., and Lieberman, M. A., 1992, *Regular and Chaotic Dynamics*, 2nd Ed., Springer-Verlag, New York.

Or, A. C., 1991, "Resonances in the Despin Dynamics of Dual-Spin Spacecraft," *Journal of Guidance, Control, and Dynamics*, Vol. 14, No. 2, pp. 321–329.

Palis, J., and Takens, F., 1993, *Hyperbolicity and Sensitive Chaotic Dynamics at Homoclinic Bifurcations*, Cambridge University Press, New York.

Rahn, C. D., and Barba, P. M., 1991, "Reorientation Maneuver for Spinning Spacecraft," *Journal of Guidance, Control, and Dynamics*, Vol. 14, No. 4, pp. 724–728.

Rimrott, F. P. J., 1989, *Introductory Attitude Dynamics*, Springer-Verlag, New York.

Rubanovskii, V. N., 1988, "On the Relative Equilibria of a Satellite-Gyrostat, Their Branchings and Stability," *Journal of Applied Mathematics and Mechanics*, Vol. 52, No. 6, pp. 710–714.

Wiggins, S., 1990, *Introduction to Applied Nonlinear Dynamical Systems and Chaos*, Springer-Verlag, New York.

Wolfram, S., 1991, *Mathematica: A System for Doing Mathematics by Computer*, 2nd Ed., Addison-Wesley, Redwood City, CA.

Ziglin, S. L., 1982, "Splitting of Separatrices, Branching of Solutions and Nonexistence of an Integral in the Dynamics of a Solid Body," *Transactions of the Moscow Mathematical Society*, Issue 1, pp. 283–298.

Transactions of the ASME®

Journal of Applied Mechanics

Published Quarterly by The American Society of Mechanical Engineers

VOLUME 63 • NUMBER 2 • JUNE 1996

Transactions of the ASME, Journal of Applied Mechanics (ISSN 0021-8936) is published quarterly (Mar., June, Sept., Dec.) for $210.00 per year by The American Society of Mechanical Engineers, 345 East 47th Street, New York, NY 10017.

Second class postage paid at New York, NY and additional mailing office. POSTMASTER: Send address changes to Transactions of the ASME, Journal of Applied Mechanics, c/o THE AMERICAN SOCIETY OF MECHANICAL ENGINEERS, 22 Law Drive, Box 2300, Fairfield, NJ 07007-2300.

CHANGES OF ADDRESS must be received at Society headquarters seven weeks before they are to be effective. Please send old label and new address. **PRICES:** To members, $40.00, annually: to nonmembers, $210.00. Add $30.00 for postage to countries outside the United States and Canada.

TECHNICAL PAPERS

(Contents continued on Outside Back Cover)